Supplementary Material

Supplementary Figure S1. PDB accession codes of all test cases, divided into those that were solved successfully and others.

Structures that successfully solved	Structures that were not successfully solved
1EJG 1EW4 1EZJ 1FK5 1G2R 1G6U 1GK6 1GVD 1GXU 1I2T 1J8B 1OAP 1OKS 1OX3 1Q8D 1R6J 1R7J 1RIY 1RW1 1T07 1TGR 1U84 1UJ8 1USE 1USM 1V2Z 1V70 1VBW 1VJK 1WHZ 1WPA 1Y0N 1Y6X 1YIB 1YU5 1YZM 1Z0P 1Z96 1ZVA 1ZZK 2B8I 2C60 2CWY 2D3D 2EFV 2ES9 2F60 2FI0 2FQ3 2FU2 2G7O 2GKR 2GPI 2H9U 2HDZ 2HL7 2HPJ 2I4A 2IGP 2IP6 2JKU 2NML 2NS0 2NUH 2O1K 2O37 2O4T 2OQQ 2OUF 2OVG 2OXO 2P5K 2P6V 2PST 2Q2F 2QFF 2QMT 2QSB 2QVO 2QYW 2RFF 2RHF 2V75 2VC8 2VKL 2YZT 2ZQE 2ZQM 3A4C 3ADG 3B64 3BJO 3BN0 3BRI 3C0F 3CE7 3CEC 3CQ1 3DF8 3E21 3EFG 3F2E 3FBL 3FF5 3FKC 3FMY 3FT7 3G21 3G2B 3GOE 3H01 3H36 3H8H 3HGL 3HRO 3HZ7 3IDW 3IM3 3JTZ 3JVL 3K3V 3KW6 3LAX 3LBJ 3MWZ 3MXZ 3NRW 3OOU	1EN2 1F94 1GMX 1I71 1IQZ 1J2L 1J8E 1KTH 1KWI 1L9L 1LSL 1LXJ 1M1Q 1MG4 1MK0 1NE8 1NJH 1NNX 1P9G 1PZ4 1RLK 1RWJ 1SBX 1TG0 1TS9 1TTZ 1TUK 1TUW 1U2H 1U3Y 1U9P 1UB9 1UCS 1UOY 1V05 1VYI 1WRI 1XAK 1XBI 1XE1 1XG8 1XW3 1Y9L 1YGT 1Z21 1ZLD 1ZT3 2ASC 2B1Y 2BKF 2BRF 2CBO 2CG7 2CMP 2CWR 2CYJ 2D9R 2E3H 2EA9 2EWH 2EWK 2EWT 2FB6 2FHT 2GYZ 2H8E 2HAZ 2HC8 2HLR 2I5F 2I6V 2IAY 2IVY 2J6B 2J8B 2J97 2NQW 2NSC 2O0Q 2O9U 2OD5 2OOA 2OQK 2PK8 2PND 2PPN 2PY0 2Q79 2QSK 2QTD 2R39 2R4Q 2RH2 2RIL 2UUX 2VQ4 2VSD 2WBX 2WJ5 2WKD 2WUJ 2X3G 2XFD 2XNQ 2YV4 2YVI 2YXF 2ZXY 3A0S 3A38 3AGN 3BN7 3BT4 3BV8 3CA7 3CI9 3CTR 3CW3 3DML 3DQY 3E0E 3E56 3E9V 3EAZ 3EMI 3ENU 3EWG 3EXY 3F14 3F40 3FDR 3FF2 3FFY 3GHF 3GV3 3H9W 3HMS 3HNX 3HQX 3HRL 3I8Z 3IV4 3JSC 3JSR 3JU3 3K0X 3KKF 3KP8 3KZD 3L32 3L4H 3L9A 3LDC 3LE4 3LWC 3LYG 3LYW 3MSH 3N3F 3NBM 3NGG 3NPD 3NX6 3NZL 3OIZ 3OSH 3PHN

Supplementary Figure S1. The relationship between top SPICKER cluster size and the success or failure of MR attempts on derived search models.

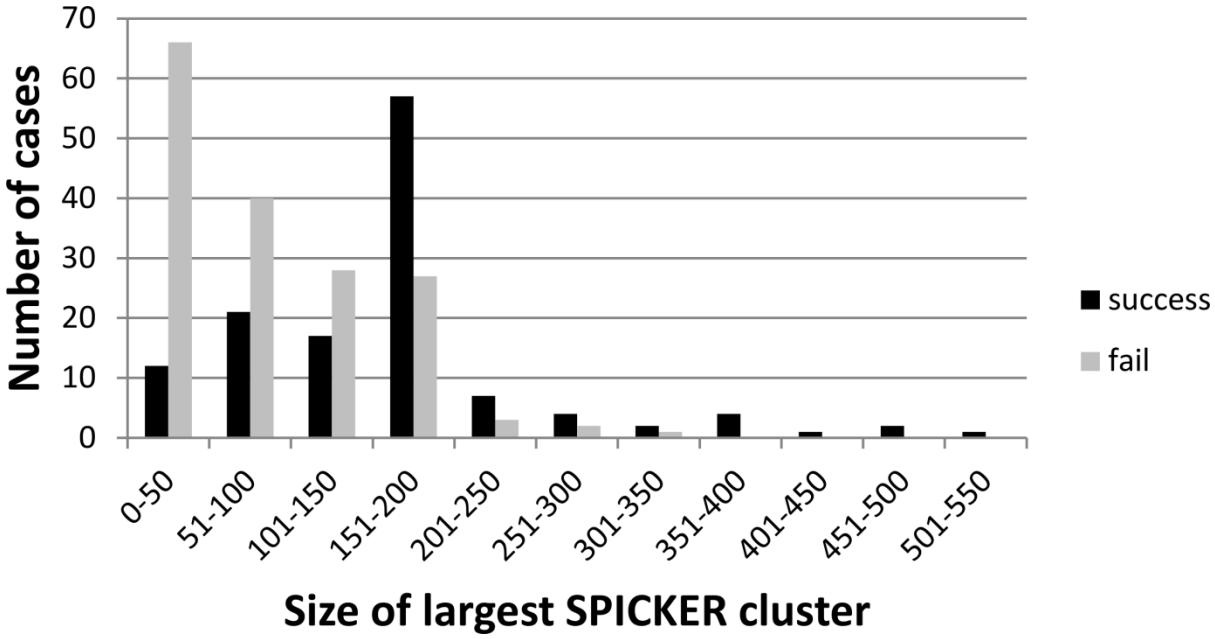

Supplementary Figure S2. Examples of how progressive truncation of ensembles results in reductions of the rmsd values of the resulting structural cores with respect to experimental crystal structures. The rmsd values are measured for search models post-MR, with both PHASER and MOLREP, and after brief refinement in REFMAC. Search models for targets 1G6U and 1R6J are shown with ultimately successful solutions shown in black. Success is not achieved until inaccurate regions have been removed.

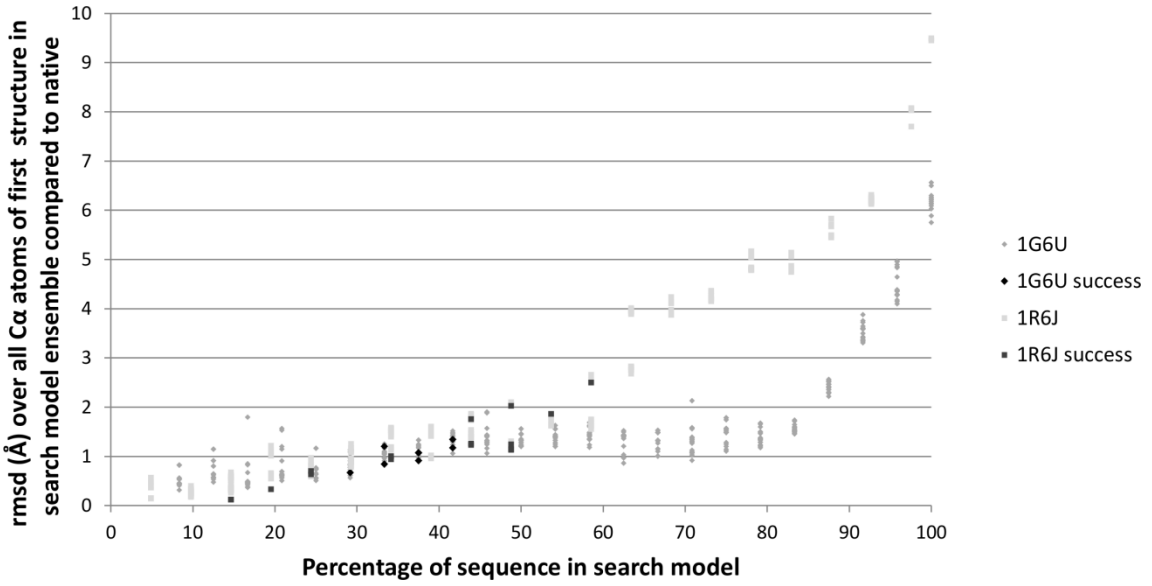

Supplementary Figure S3. Distribution of SHELXE CC scores after density modification and main-chain tracing. The peak on the right with scores greater than 25% contains correct solutions that can be automatically traced.

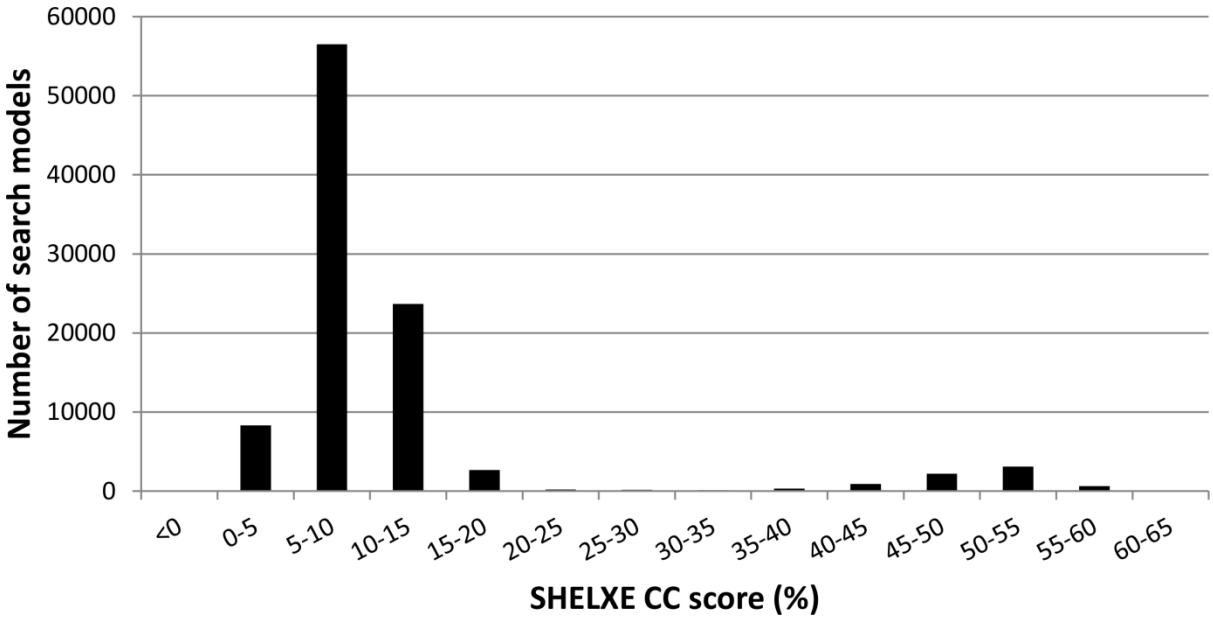

Supplementary Figure S4. Relationships between a) SHELXE CC score and Reforigin rmsd, b) SHELXE CC score and Rfree and c) rmsd error of model and Reforigin *rmsd* for successful search models. a) illustrates that, as expected, accurate placement of the search model is generally required for success, although in a surprisingly large number of cases wholly inaccurate placement that resulted in the fortuitous matching of some secondary structure elements yielded sufficient phasing power for refinement. c) indicates that successes from inaccurate placement arise for both accurate and inaccurate models.

A)

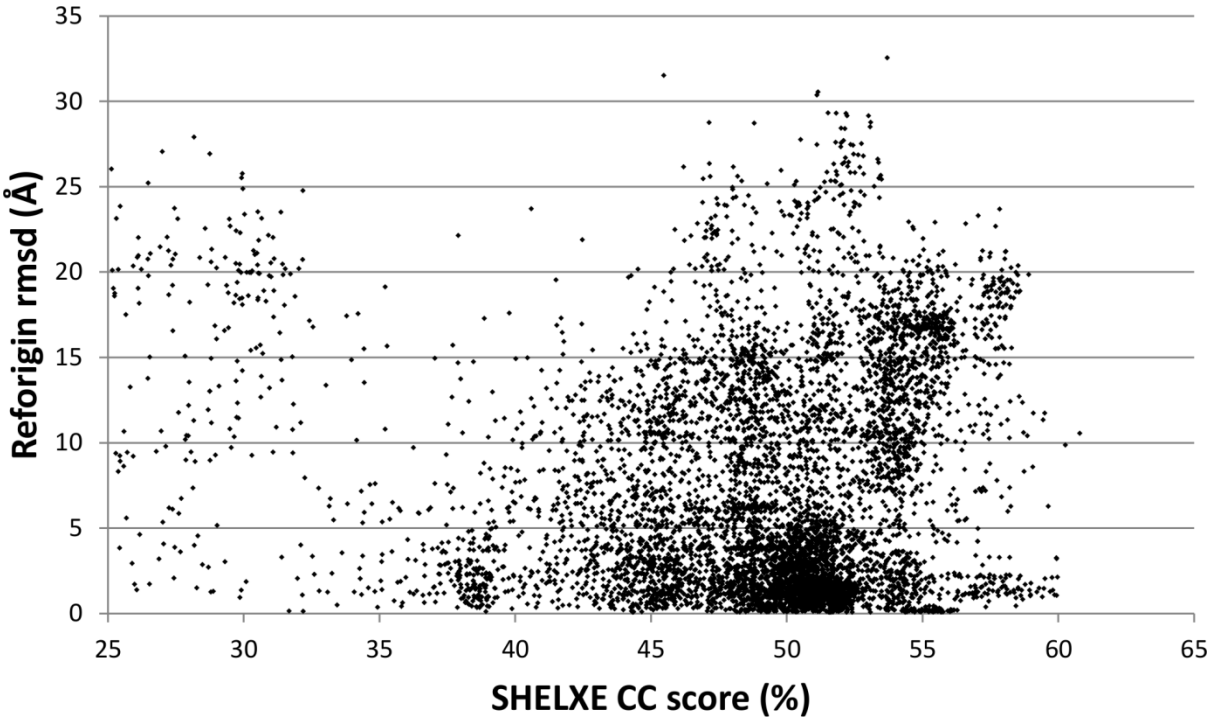

B)

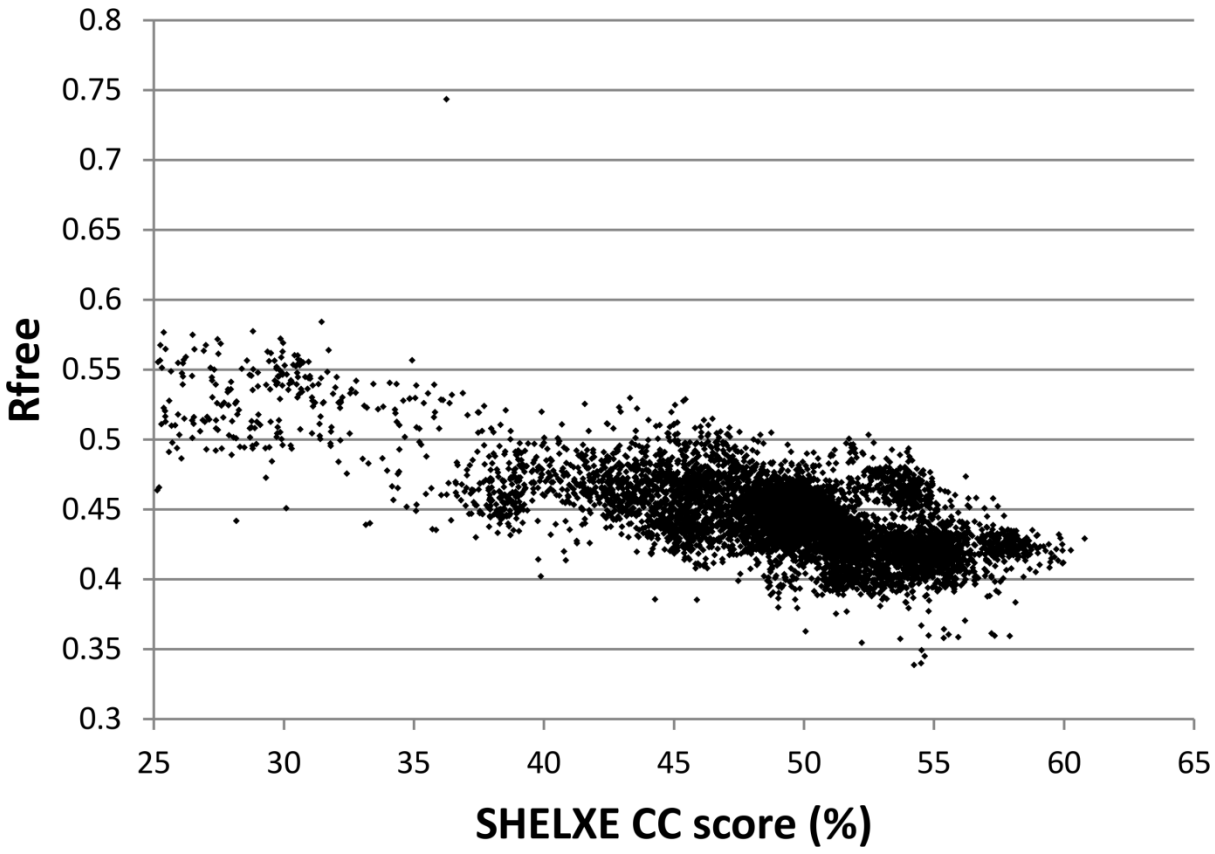
0.8
0.75
0.7
0.65
0.6
0.55
0.5
0.45
0.4
0.35
0.3
Rfree
25
30
35
40
45
50
55
60
65
SHELXE CC score (%)

C)

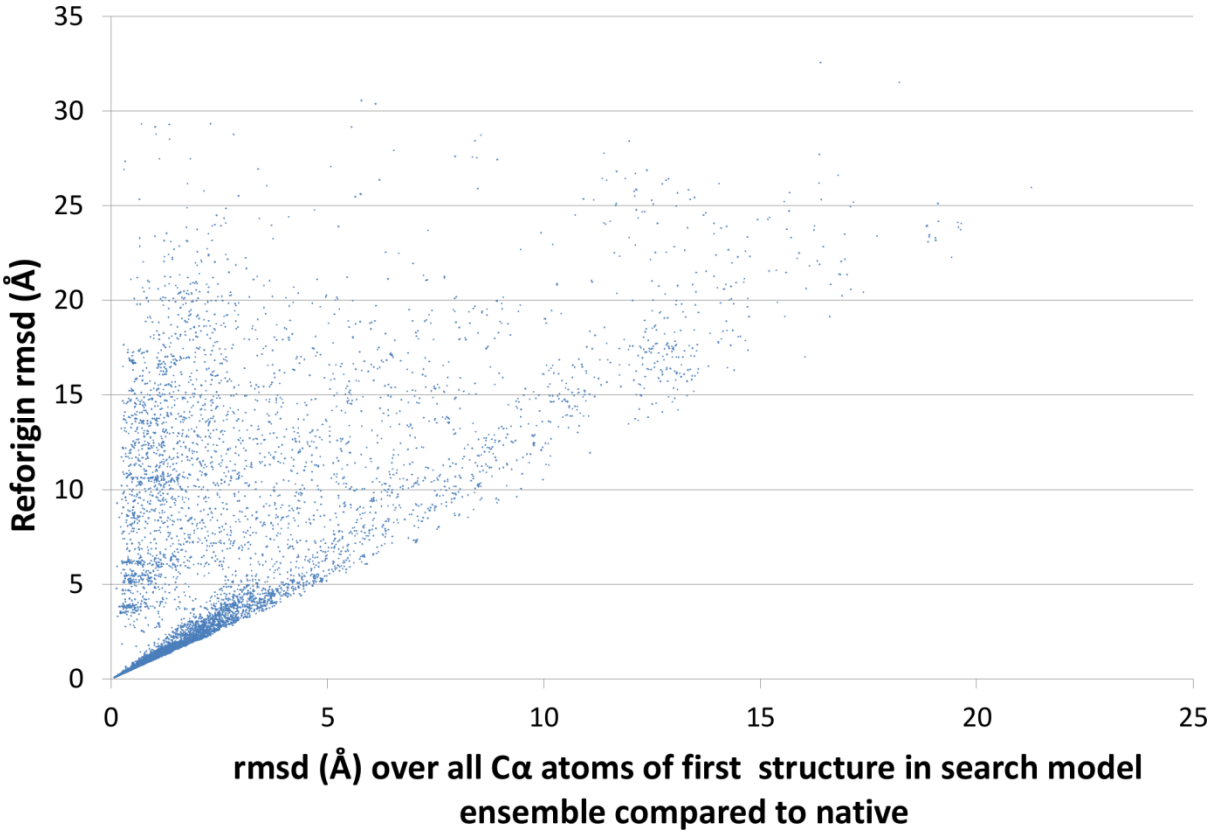
35
30
25
20
15
10
5
0
Reforigin rmsd (Å)
0
5
10
15
20
25
rmsd (Å) over all Cα atoms of first structure in search model ensemble compared to native

Supplementary Figure S5. Phaser TFZ scores for successful and unsuccessful search models. The failures in the most populated bins number 2961 (TFZ 2-3), 12081 (3-4), 17956 (4-5) and 5636 (5-6).

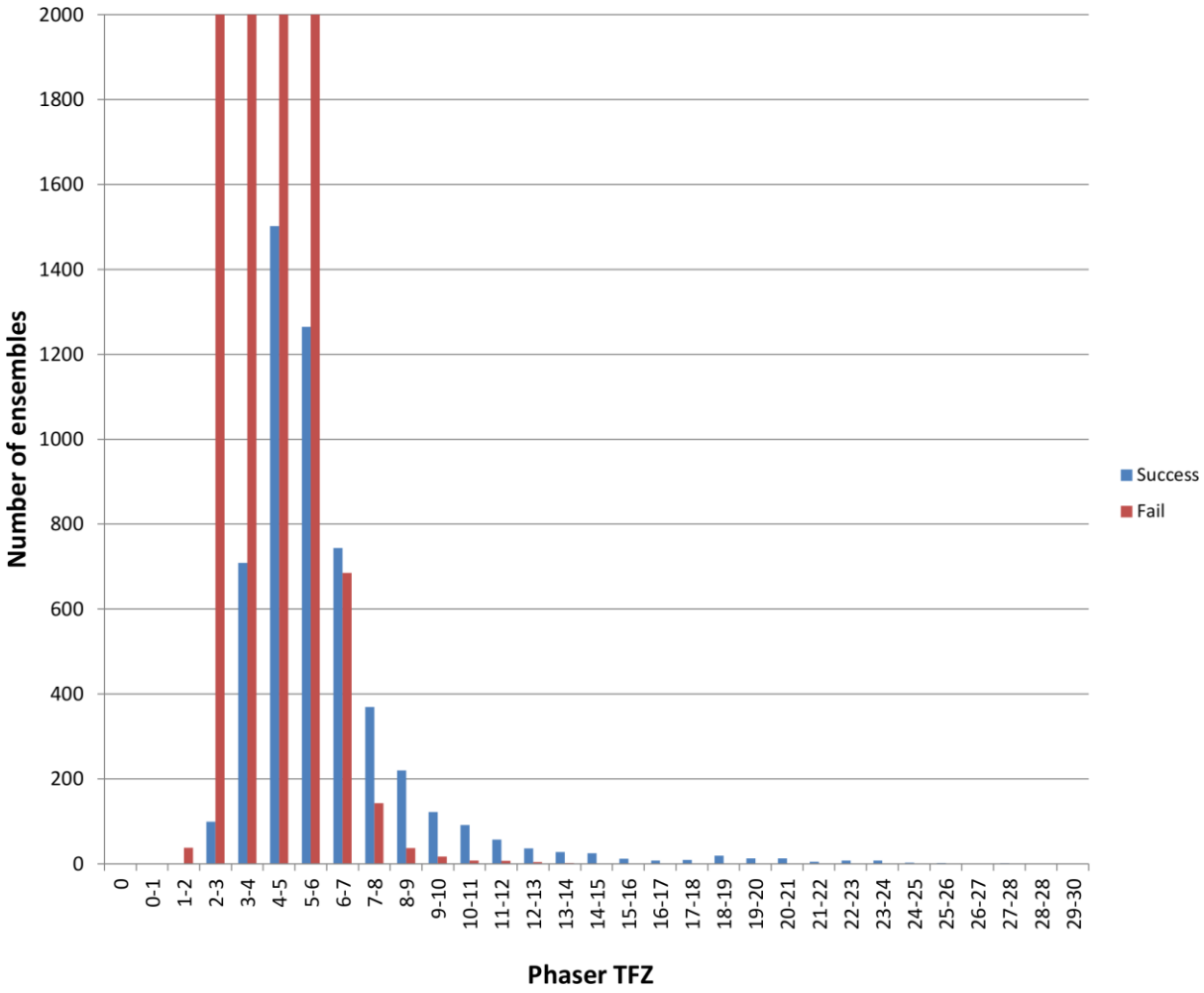

Supplementary Figure S6. All-α targets are more accurately modelled than all-β targets, with mixed α-β targets intermediate. The bar charts show, for each fold class, the mean GDT score of the best decoy produced by ROSETTA for each target.

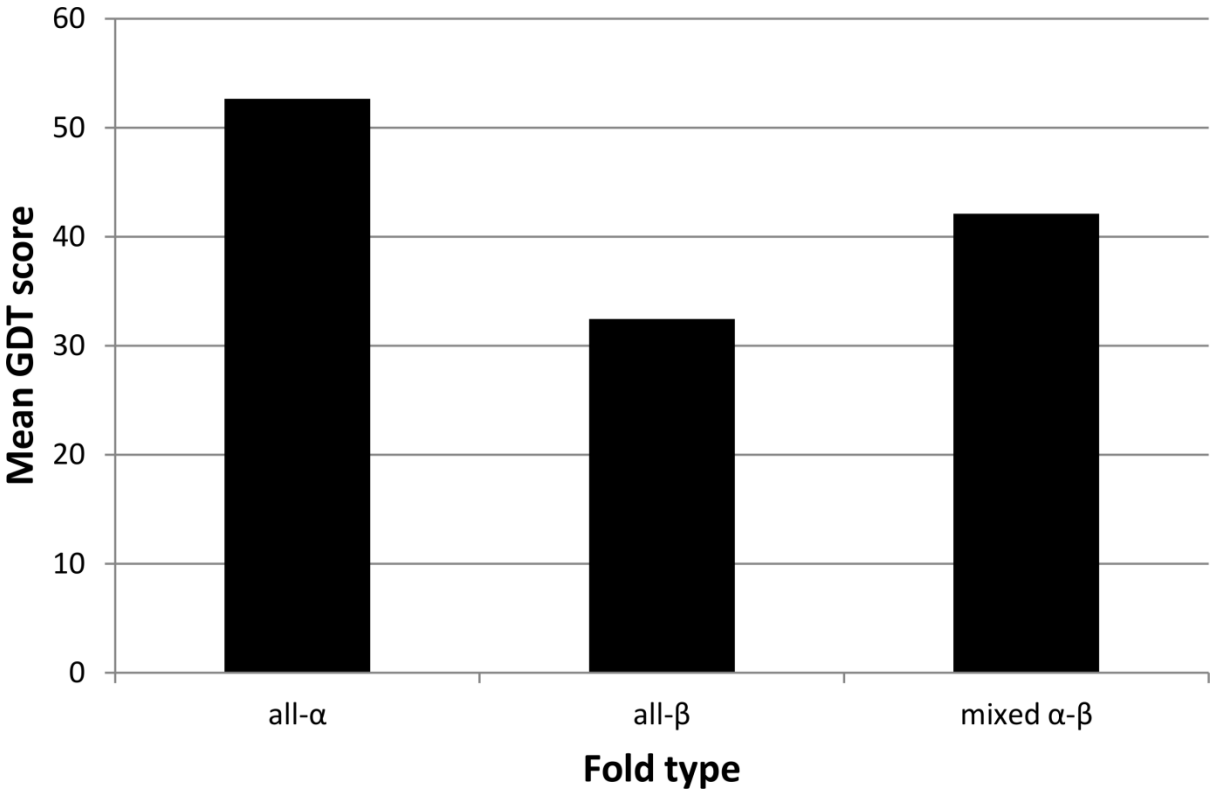

Supplementary Figure S7. The crystal system of the target structure has little influence on success. Bars show numbers of successful cases in each category topped by the % of targets that were successful.

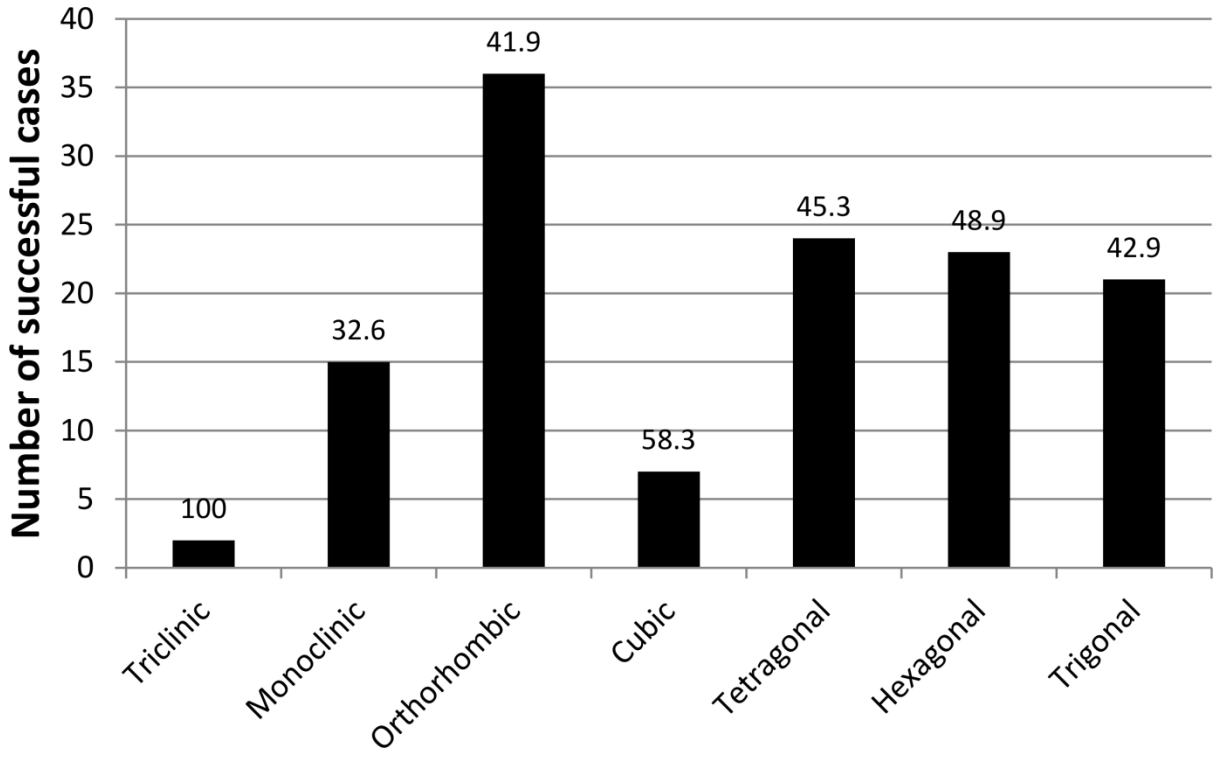

Supplementary Figure S8. The % solvent content of target crystal structure has little influence on success. Bars show numbers of successful cases in each range topped by the % of targets that were successful.

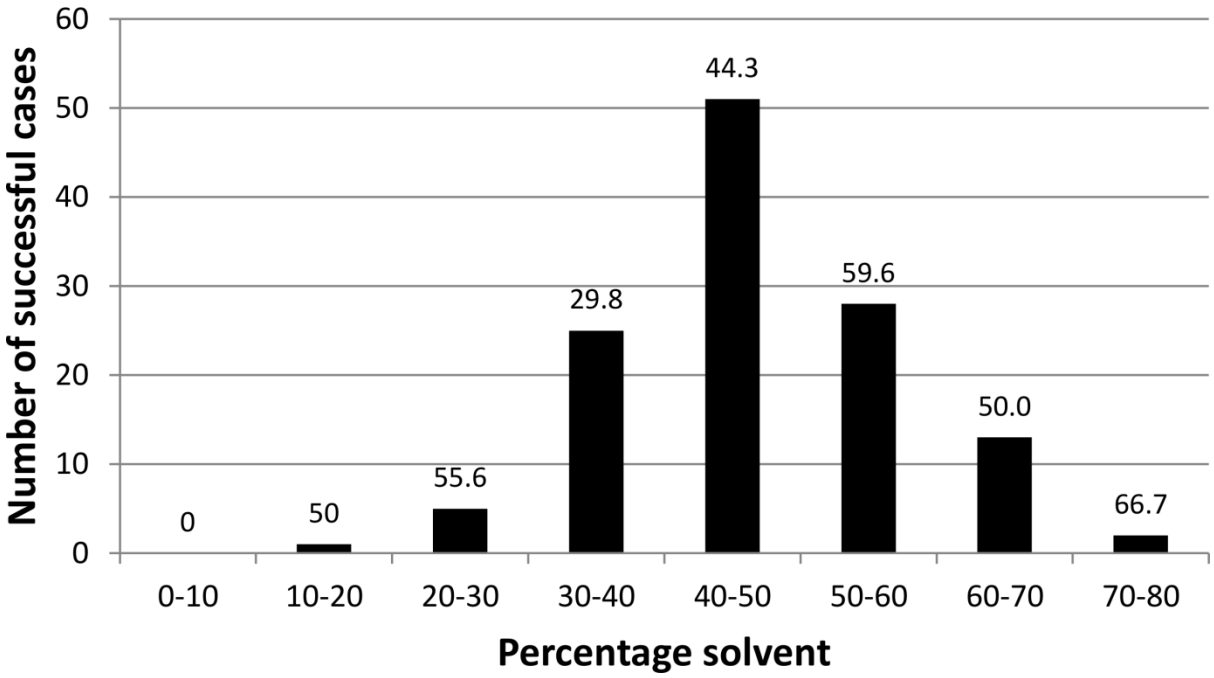

Supplementary Figure S9. In the range covered here, the high resolution limit of the diffraction data appears to have little influence on success. Bars show numbers of successful cases in each range topped by the % of targets that were successful.

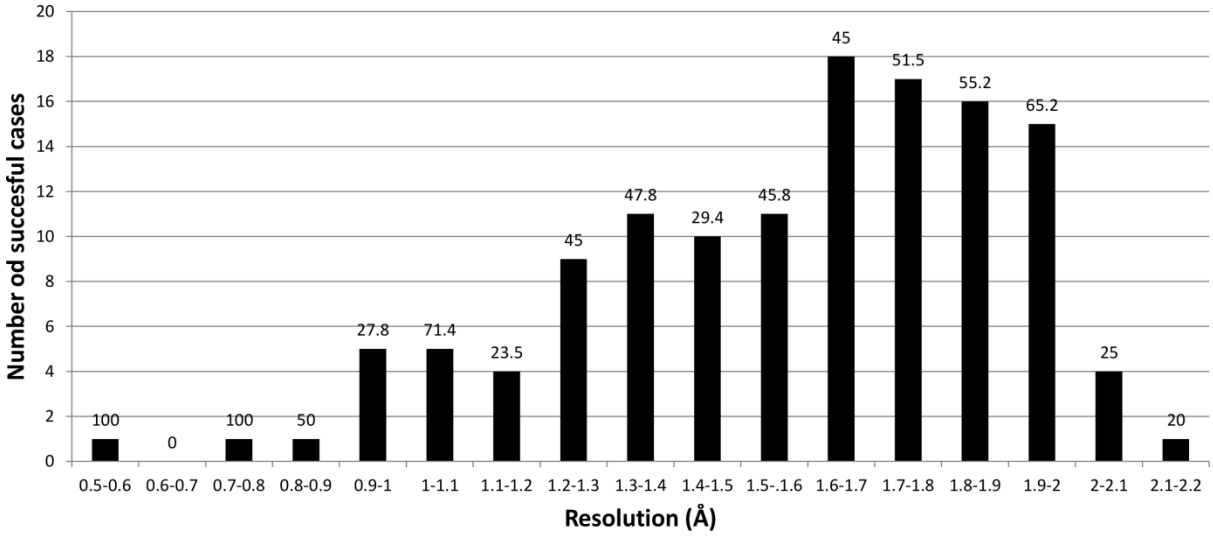

Supplementary Figure S10. Success is more likely when the initial SPICKER clusters contain decoys with a GDT score of greater than 40 i.e. with an approximately correct overall fold. Black bars are cases where search models deriving from SPICKER cluster 1 were successful. Dark grey shows cases that solved with cluster 2 but not cluster 1. Scores for cluster 1 of failing targets are shown in light grey.

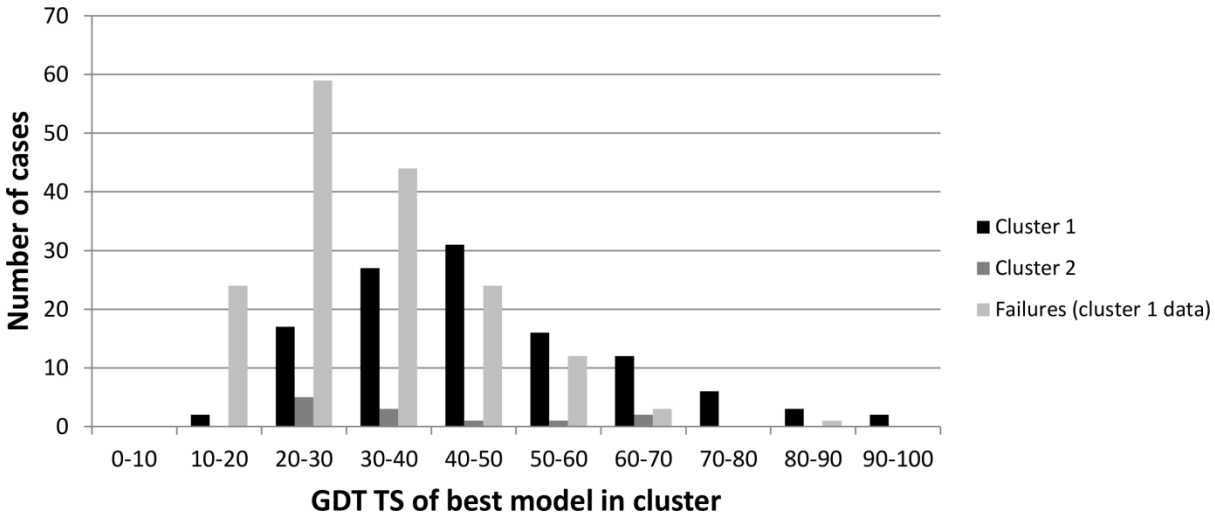

Supplementary Figure S11. Representative examples of accurately modelled ensembles of different sizes that successfully solved their targets. a) a 4 residue (5%) fragment of target 1ZZK with rmsd error 0.14 Å and reforigin value of 3.3 Å, b) a 31 residue (40%) region of 1USM (rmsd 0.7 Å, reforigin 0.8 Å) and c) a full-length, 116 residue model ensemble of 3MXZ (rmsd 5.7 Å, reforigin 6.3 Å). In each case the target is shown coloured blue to red, from N- to C-terminus, and the search model shown in pink.

a)

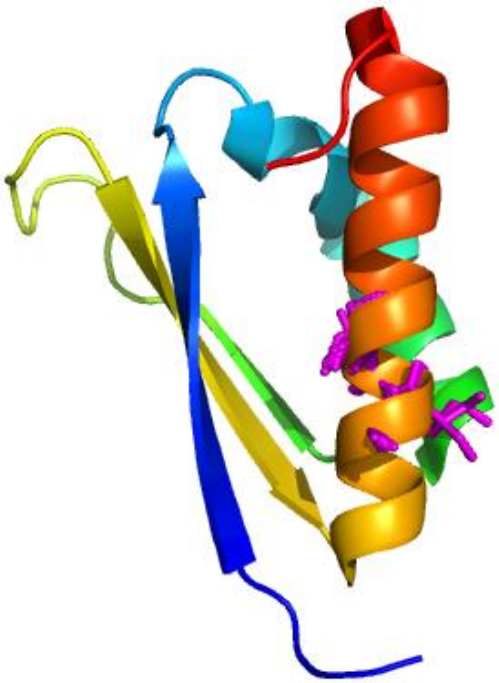

b)

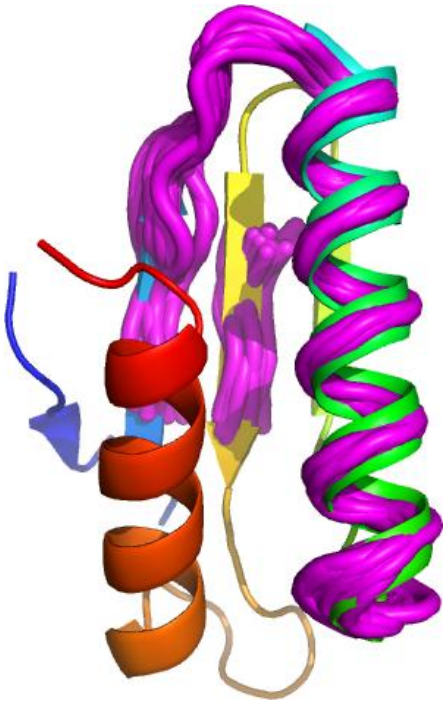

c)

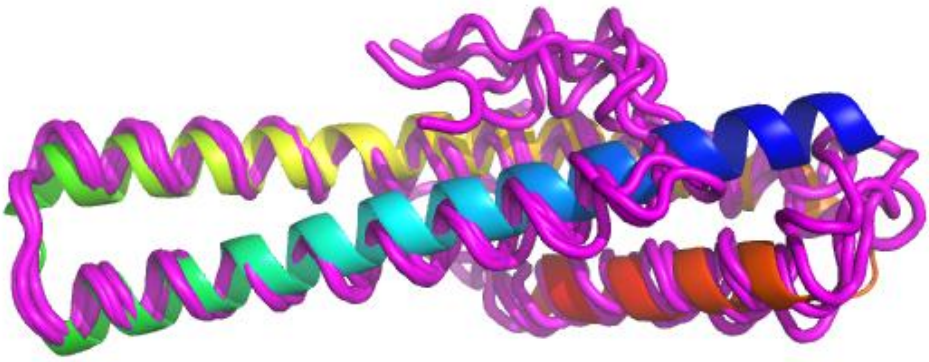

Supplementary Figure S12. Examples of successes arising from inaccurately modelled and/or inaccurately placed search models. Such cases occur predominantly for targets with long α-helices. a) target 1GK6 with rmsd error 21.3 Å and reforigin value of 26.0 Å, b) 3EFG (rmsd 16.6 Å, reforigin 19.1 Å), c) 2ZQM (rmsd 2.3 Å, reforigin 29.3 Å) and d) 1WPA (rmsd 2.1 Å, reforigin 26.0 Å). Colouring is as in Figure S11

a)

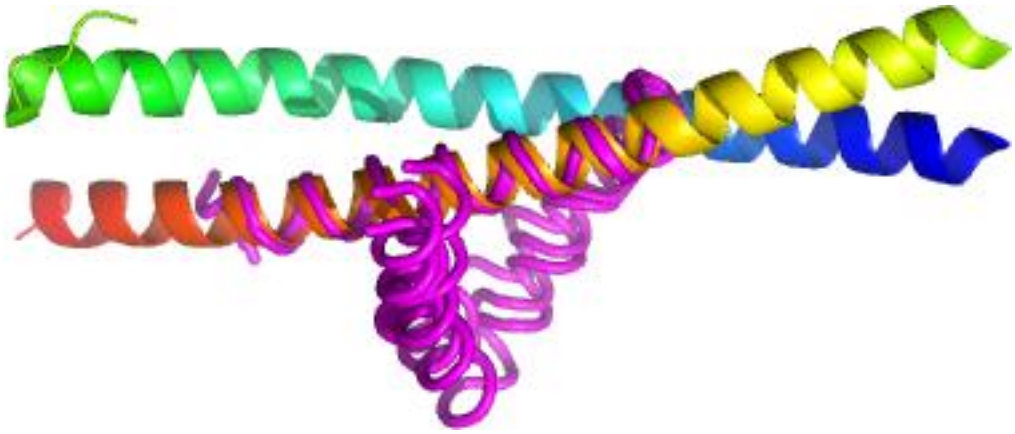

b)

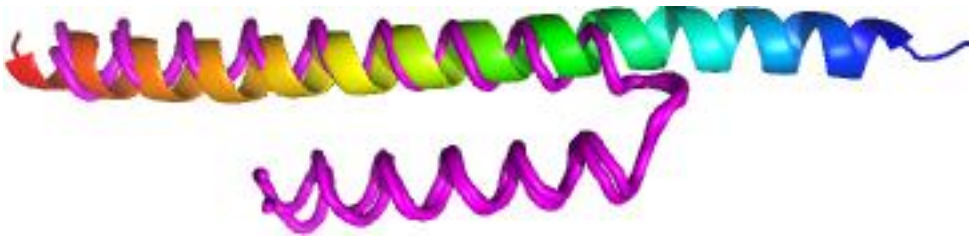

c)

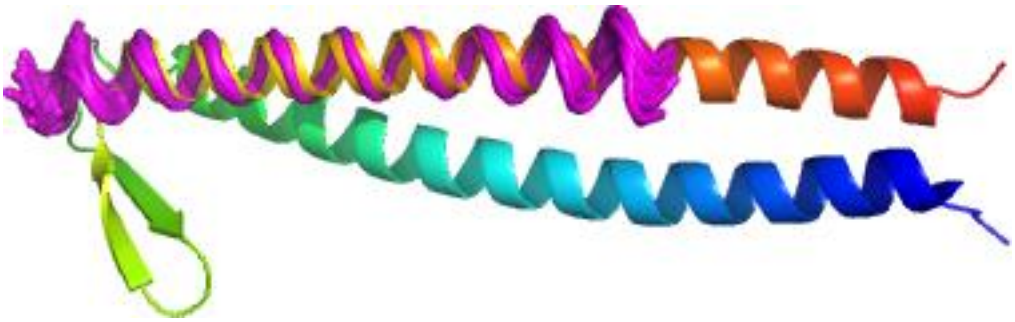

d)

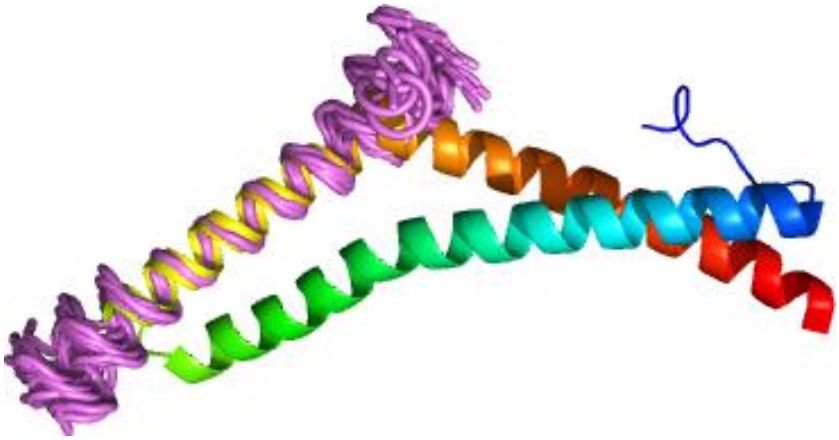
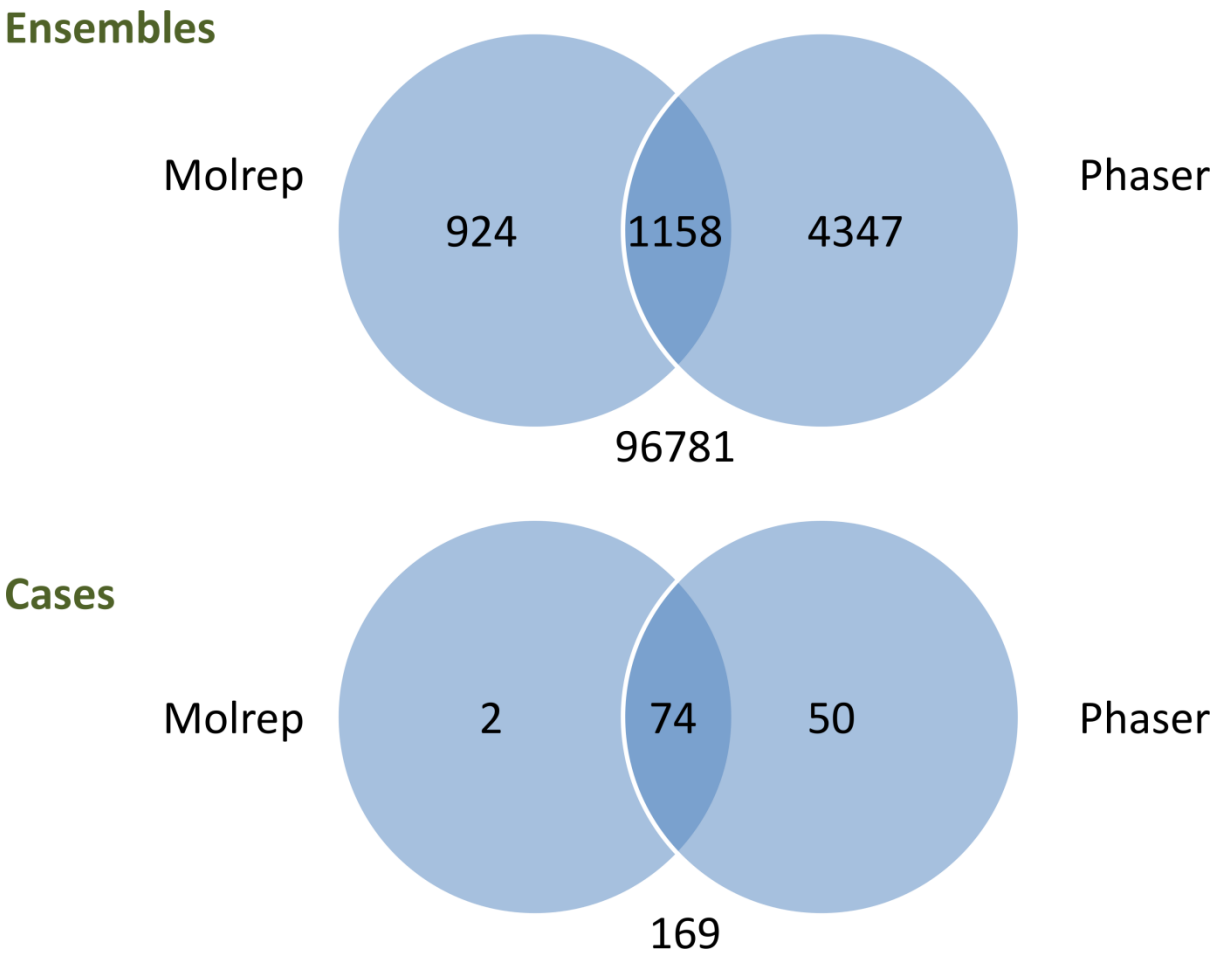
Supplementary Figure S13. Venn diagrams illustrating ensembles (above) and targets (below) that could be solved by PHASER, by MOLREP, by both or by neither.